American Journal of Pathology, Vol. 157, No. 4, October 2000

Short Communication

Enhancement of Chemical Hepatocarcinogenesis by the HIV-1 *tat* Gene

Giuseppe Altavilla,* Antonella Caputo,† Massimo Lanfredi,† Catia Piola,‡ Giuseppe Barbanti-Brodano,† and Alfredo Corallini†

From the Institute of Pathologic Anatomy and Histology, University of Padova, Padova; the Department of Experimental and Diagnostic Medicine,† Section of Microbiology and the Interdepartment Centre for Biotechnology,‡ University of Ferrara, Ferrara, Italy*

The human immunodeficiency virus-1 Tat protein is suspected to be involved in the neoplastic pathology arising in AIDS patients. *tat*-transgenic (TT) mice, which constitutively express Tat in the liver, develop liver cell dysplasia (LCD) that may represent a preneoplastic lesion. To test if TT mice are predisposed to liver carcinogenesis, we treated them with diethylnitrosamine, a hepatotropic carcinogen. Diethylnitrosamine-treated TT mice developed both preneoplastic and neoplastic lesions in the liver. They showed an enhancement of LCD and developed basophilic liver cell nodules (BLCN), hepatocellular adenomas (HA), and hepatocellular carcinomas (HC). Both preneoplastic (LCD and BLCN) and neoplastic (HA and HC) lesions were significantly more frequent in TT than in control mice: 29.7% *versus* 12.7% for LCD, 57.9% *versus* 23.3% for BLCN, 40.6% *versus* 10.0% for HA, and 50.0% *versus* 12.7% for HC. These results indicate that Tat expression in the liver predisposes to both initiation of hepatocarcinogenesis and to malignant progression of liver tumors. This study supports a role for Tat in enhancing the effect of endogenous and exogenous carcinogens in human immunodeficiency virus-1-infected patients, thereby contributing to tumorigenesis in the course of AIDS. *(Am J Pathol 2000, 157:1081–1089)*

Human immunodeficiency virus type-1 (HIV-1) infection and AIDS are associated to an opportunistic pathology, which includes various types of tumors.[1–3] These neoplasms are mainly determined by the state of severe immunodeficiency accompanying HIV-1 infection and AIDS, as a consequence of elimination of the immunosurveillance on tumor formation. Other factors, however, may participate in AIDS-associated oncogenesis. The HIV-1 Tat protein, that is secreted by HIV-1-infected cells[4,5] and taken up by normal cells,[6,7] is a likely candidate to contribute to tumor pathogenesis in HIV-1-infected patients, because of its growth-promoting activity, angiogenic functions, and anti-apoptotic effect.[8–13] The oncogenic role of Tat is supported by tumorigenesis in *tat*-transgenic (TT) mice.[14–16] BKV/TT mice, where the *tat* gene is expressed in all organs and tissues,[15,16] develop preneoplastic and neoplastic lesions closely mimicking those appearing during HIV-1 natural infection, namely skin angiogenic lesions resembling the early stages of Kaposi's sarcoma, B-cell lymphomas, skin papillomas, squamous cell carcinomas and leiomyosarcomas, adenocarcinomas of skin adnexa, rectum polyps, and hepatocellular carcinomas (HCs).[15,16]

Although the incidence of HC is low, most animals show a liver cell dysplasia (LCD) of variable degree.[15,16] It is likely that LCD in TT mice represents a preneoplastic lesion which can be assumed as a model to test the role of *tat* in predisposition to tumor formation in HIV-1-infected patients. Predisposition to chemical carcinogenesis has been demonstrated in mice transgenic for the hepatitis B virus genome[17] and for a mutant p53 gene[18] as well as in knock-out mice nullizygous for p53.[19] We therefore treated BKV/TT mice with diethylnitrosamine (DENA), a hepatotropic carcinogen, to establish whether liver carcinogenesis is enhanced compared to normal control mice. DENA is a potent initiator of carcinogenesis and induces liver cancer slowly after a single oral, intraperitoneal, or intravenous dose.[20] Twenty-four hours after DENA administration to rats, necrotic hepatocytes are readily visible, followed by proliferation of liver oval cells with restitution to the normal acinar architecture 14 days

Supported by funds from Ministero dell'Università e della Ricerca Scientifica e Tecnologica (MURST 60%, 1997 and 1998) (to G. A. and to A. C.), and from the AIDS Project of the Italian Ministry of Health (AIDS Projects 1997 and 1998, Istituto Superiore di Sanità, Rome) (to A. C.).

Accepted for publication July 12, 2000.

Address reprint requests to Dr. Giuseppe Altavilla, M.D., Institute of Pathologic Anatomy and Histology, University of Padova, Via Gabelli 61, I-35100 Padova, Italy. E-mail: altavill@ux1.unipd.it.

after carcinogen administration. However, occasional proliferation of hepatocytes with nuclear pleomorphism and basophilic cytoplasm occurs. Then, these small foci of rapidly growing altered basophilic hepatocytes expand, so that 6 weeks later many foci increase to 3 mm in diameter and HCs are detected several months after DENA administration.[21]

Materials and Methods

Transgenic Mice

The generation of transgenic BDF mice carrying BKV/*tat* sequences has been previously described.[15,16] Seven founder mice were identified, each giving rise to a transgenic mouse line by crossing initially with normal BDF mice and then with heterozygous transgenic mice of the same lineage to obtain animals homozygous for the transgene.

Induction of Tumors

Eighty-nine TT mice and 200 BDF normal controls (CC) were injected intraperitoneally with DENA (Sigma, St. Louis, MO) dissolved in physiological saline according to the protocol of DENA carcinogenesis reported by Vesselinovich and Mihailovich.[22] We performed two experiments to assess the effects of different doses of DENA. In experiment 1, 64 TT and 150 CC mice were treated with two injections of DENA, the first at day 7, the second at day 14 after birth. The total dose of DENA injected was 15 mg/kg body weight. To confirm the results of the first experiment, a second experiment was performed in which only one injection of DENA was given to 25 TT and 50 CC mice at day 10 after birth. The total dose of DENA injected was 7.5 mg/kg body weight.

Animal Examination

Animals were routinely examined twice a week for the appearance of symptoms. Groups of TT and CC animals were sacrificed at regular intervals, that is at 100, 200, 300, 400 and 600 days after injection of DENA. All mice, either dead by natural causes or sacrificed, were subjected to autopsy.

Histological and Histochemical Procedures

Tissue samples from all organs taken at autopsy were fixed in 10% phosphate-buffered formalin for 12 to 24 hours and embedded in paraffin for histological and histochemical examination. At least two representative fragments of each lobe of the liver were taken: one of these was cryopreserved at −80°C for molecular studies, whereas the other was subjected to histological and histochemical analysis. Three- to five-μm serial sections were stained with hematoxylin and eosin for the histological examination and with periodic acid-Schiff (Merck, Frankfurt, Germany), with and without Diastase (Sigma) pretreatment for the assessment of the glycogen content of liver cells. For the histochemical analysis of CD19, CD20, CD21, and CD45R B cell markers, after removal of paraffin and rehydration and after block of the endogenous peroxidases with 0.3% H_2O_2 in methanol, the samples were incubated with mouse antibodies for 10 to 12 hours at 4°C. Then anti-mouse immunoglobulins (DAKO, Glostrup, Denmark) were used as secondary antibodies followed by incubation with avidin-biotin-peroxidase conjugates and development in diaminobenzidine (Sigma).[16]

Electron Microscopy

For ultrastructural investigations, specimens of liver tumors and nodules were fixed with glutaraldehyde in phosphate-buffered saline (PBS) (0.2 mmol/L, pH 7.2) for 8 hours, postfixed in 1% OsO4 in PBS for 4 hours, dehydrated, and embedded in Araldite. Ultrathin sections were stained with uranyl acetate and lead citrate and were examined with a Hitachi H-7000 electron microscope.

Morphological Criteria Used for the Classification of Liver Lesions

The criteria of Koen et al[23] and Becker,[24] slightly modified, were used for the classification of liver lesions. He-

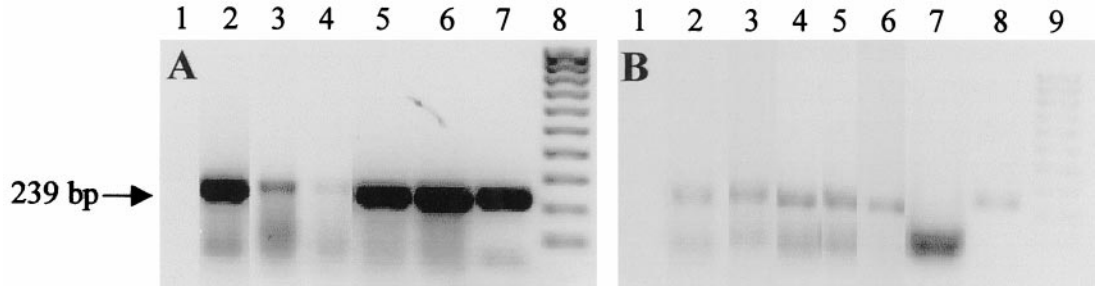

Figure 1. Analysis of *tat* DNA (**A**) and RNA (**B**) by PCR and RT-PCR. After DNA amplification, the samples were run in agarose gel electrophoresis and stained by ethidium bromide. **A: Lane 1**, negative control; **lanes 2** and **3**, LCD; **lane 4**, BLCN; **lane 5**, HA; **lane 6**, HC; **lane 7**, T53 cell line constitutively expressing *tat*; **lane 8**, molecular weight markers XIV (Boehringer). **B: Lane 1**, negative control, **lanes 2** and **3**, LCD; **lane 4**, BLCN; **lane 5**, HA; **lanes 6** and **7**, HC treated and untreated with reverse transcriptase, respectively; **lane 8**, T53 cell line constitutively expressing *tat*; **lane 9**, molecular weight markers XIV (Boehringer). The band of 239 bp (**arrow**) is the *tat* amplification product. The lower band represents the primers which migrated at the bottom of the gel.

patocyte proliferative lesions >1 mm were defined as liver tumors[24] and classified as adenomas or carcinomas based on cytological features and architectural patterns. The LCD and basophilic liver cell nodules (BLCN) were identified according to Solt et al[21] Similar cytological modifications associated with other pathological conditions (inflammation, amyloidosis) of the liver were not considered as dysplastic-preneoplastic lesions and were not included in our analysis. All of the proliferative liver lesions were grouped as follows: LCD, BLCN, hepatocellular adenoma (HA), and HC.

Nucleic Acid Hybridization, Polymerase Chain Reaction (PCR), and Reverse Transcriptase-Polymerase Chain Reaction (RT-PCR)

DNA and RNA extraction, and nucleic acid hybridization were performed according to standard techniques.[25] *tat* cDNA labeled with ^{32}P-dCTP by nick-translation or by primer extension was used as a probe. The specific activity of the probes was 1 to 6×10^9 cpm/μg. PCR and RT-PCR for *tat* cDNA and RNA were performed as previously described.[15] DNA (0.2 μg) was amplified in a DNA thermal cycler (Perkin-Elmer, Forster City, CA) in a total volume of 50 μl containing 10 mmol/L Tris-HCl, pH 8.3, 50 mmol/L KCl, 1.5 mmol/L $MgCl_2$, 100 μmol/L of each dNTP, 25 μmol/L of each primer, and 5 units of *Taq*I-DNA polymerase (Boehringer, Mannheim, Germany). A 21-mer oligonucleotide (5′GAAGCATCCAGGAAGTCAGCC3′) and a 24-mer oligonucleotide (5′ACCTTCTTCTTCTATTCCTTCGGG3′) were used as forward and reverse primers, respectively, to amplify a 239-bp sequence of *tat* cDNA. Conditions of amplification were: denaturation at 94°C for 1 minute, annealing at 55°C for 2 minutes, extension at 72°C for 2 minutes for 30 cycles with a final extension at 72°C for 10 minutes. PCR products were analyzed by electrophoresis onto a 2% agarose gel. For RT-PCR, 3 to 5 μg of total RNA were treated with 5 U of RNase-free DNase (Promega, Madison, WI) at 37°C for 20 minutes, followed by phenol-chloroform extraction and ethanol precipitation. Reverse transcription was performed with the cDNA Cycle Kit from Invitrogen (San Diego, CA) and the resulting cDNA was amplified by PCR as described above.

Statistical Analysis

Statistical differences between groups of animals were analyzed by the Fisher exact probability test. The significant level was defined at a P value < 0.05.

Results

Presence and Expression of tat cDNA in Liver Tumors

By Southern blot hybridization analysis we confirmed previous results,[15,16] namely that all tissues and organs of BKV/TT mice contain the transgene as tandem insertions in a variable number of copies (5 to 20) per cell (data not shown). Then, by PCR and RT-PCR we tested the presence of *tat* DNA and RNA in two dysplastic lesions, one basophilic liver cell nodule, one hepatoma, and one HC. The results of the analysis indicated that *tat* DNA is present and *tat* RNA is expressed in these tissues (Figure 1, A and B).

Lesions Developed in TT and CC mice

All 89 (100%) TT animals (64 of the first experiment and 25 of the second experiment) were affected with lesions when examined at autopsy. Of the 200 CC mice, only 45 (30%) and 13 (26%) in the first and second experiments, respectively, showed lesions (Table 1). No significant differences in the number of lesions were found in TT and CC animals related to gender.

Types of Lesions

The total number of lesions documented in TT mice was 219, with a ratio lesion/animal of 2.46, indicating that more than one alteration could be present in the same animal. The lesions were very similar in the two experiments and distinguished in hepatic alterations and alterations of other organs, both including 1) lesions related to the carcinogenic action of DENA and 2) lesions unrelated to DENA activity but related to the transgenic status and determined by chronic infections or other causes. The following description of lesions observed during the course of these experiments in TT and CC mice is based on histological and histochemical analysis as well as on electron microscopic examination.

Hepatic Lesions

Architectural and cytological alterations observed in both experiments of the study were morphologically similar in TT and CC animals.

Liver Cell Dysplasia (LCD)

The liver presented a normal lobular architecture and the alterations consisted exclusively in cytological changes evenly and diffusely distributed. The dysplastic hepatocytes formed cell plates separated by sinusoids and showed clear or basophilic cytoplasm, central large nuclei (often twice or more than normal in size) with nuclear/cytoplasmic ratio >1 (Figure 2, A and B). LCD was significantly more frequent in TT than in CC animals in both experiments: 29.7% *versus* 12.7% in the first experiment ($P = 3.3 \times 10^{-3}$), 56.0% *versus* 12.0% in the second experiment ($P = 9.7 \times 10^{-5}$) (Table 2). Furthermore, LCD showed a significantly higher incidence in TT mice in the second experiment (56.0%) compared to the first (29.7%) ($P = 2 \times 10^{-2}$). This difference is likely because of the less severe effect of one dose of DENA in the second experiment, inducing a prevalence of the milder preneoplastic lesions.

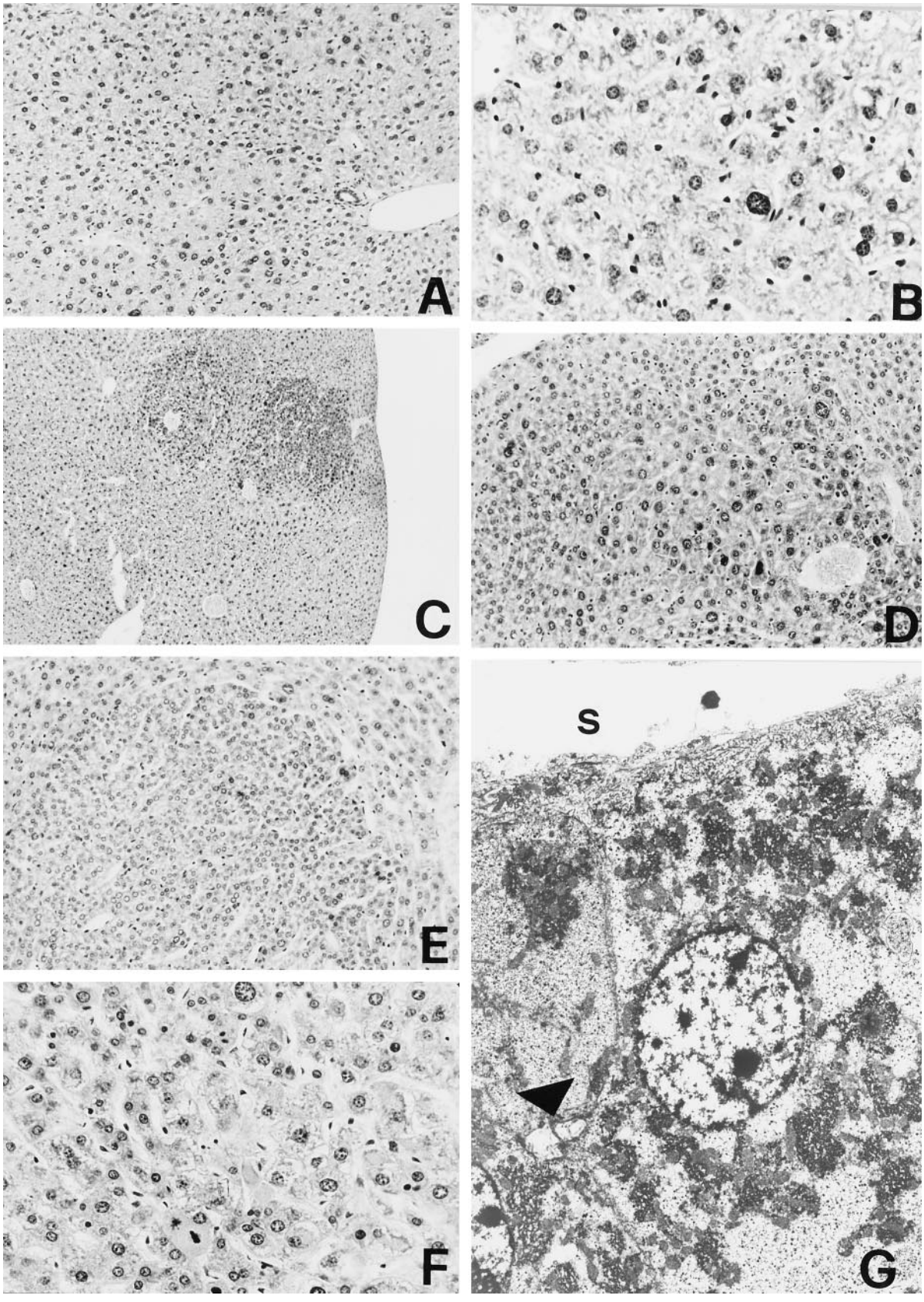
A
B
C
D
E
S
F
G

Basophilic Liver Cell Nodules (BLCN)

Although BLCN were randomly distributed, they were more often observed adjacent to centrolobular veins. Based on size or number of forming cells and architecture, BLCN were differentiated as small or large. The small BLCN consisted of 20 to 100 cells with a clear delimitation from the normal tissue. The hepatocytes were smaller than normal with more basophilic and sometimes foamy cytoplasm, large nuclei with chromatin granules, and prominent nucleoli. Mitoses were rare. The small BLCN did not contain newly formed vascular network and sinusoids appeared compressed. The large BLCN consisted of >100 cells and showed cytological characteristics similar to the small ones, but with no marked outline from normal adjacent tissue and with a more prominent variability of the nuclear size. The altered hepatocytes were aggregated in plates with more than one element in thickness, separated by sinusoids. In the largest BLCN, cell plates formed incomplete trabeculations at the periphery (Figure 2, C and D). Numerous BLCN showed intermediate features between small and large types. The frequency of BLCN was significantly greater in TT than in CC animals in the first experiment: 57.9% *versus* 23.3% ($P = 1.5 \times 10^{-6}$), whereas it was not significant in the second experiment: 36.0% *versus* 22.0% ($P = 1.5 \times 10^{-1}$) (Table 2). More than one type of BLCN was observed in the same liver and often in the same lobe. BLCN were more frequently associated with LCD and HA, and less frequently with HC.

Hepatocellular Adenomas

In this category we considered alterations that fulfilled the criteria of type I and small type II lesions of Becker's classification.[24] They appeared as nodular proliferations varying in diameter from 1 mm to >1 cm, with sharp borders and with some grade of compression of normal adjacent tissue. Small tumors were composed almost entirely of basophilic cells, but in the large tumors zones of trabeculation became more evident, extending variably from <5% to 50% of the total section and usually located in the central areas. Trabeculations in the small and large tumors were one to two cells thick (rarely three cells) separated by slit-like sinusoids lined by endothelium. They were irregularly branched and were composed of cells with basophilic cytoplasm and central oval nucleus with small nucleoli. In some instances periodic acid-Schiff-diastase-positive hyaline globules were observed in the cytoplasm. Mitoses were absent or very few (Figure 2, E–G). HA were 40.6% in TT mice and 10.0% in CC mice in the first experiment ($P = 6.6 \times 10^{-7}$). This greater incidence was confirmed in the second experiment: 32.0% in TT mice and 8.0% in CC mice ($P = 1.1 \times 10^{-2}$) (Table 2).

Hepatocellular Carcinomas

In this histotype we grouped lesions similar to the large type II, III, and IV tumors of Becker's classification.[24] Histologically HCs varied from a well-differentiated appearance to a poorly differentiated solid pattern. The well-differentiated type HCs showed trabecular structures (Figure 3A). The cell plates had a thickness of more than two to three cells and were more irregularly branched compared to HA. HCs were usually characterized by severe cellular atypia with a nuclear/cytoplasmic ratio >1, a variable nuclear size and structural abnormalities of chromatin and nucleoli. Mitotic activity was variable but always evident and greater than in HAs (Figure 3, B and D). In the poorly differentiated tumors, the trabeculae were composed of plates which were five to 10 or more cells thick, sometimes forming blunt pseudopapillary structures with cystic and necrotic areas (Figure 3C). The HCs were aggressive and invasive, because they produced lung metastases (Figure 3E). They were significantly more frequent in TT than in CC animals both in the first and in the second experiment, independently from the dose of DENA: 50.0% *versus* 12.7% in the first experiment ($P = 1.7 \times 10^{-8}$), 32.0% *versus* 4.0% in the second experiment ($P = 1.7 \times 10^{-3}$) (Table 2).

The distribution of the total liver preneoplastic and neoplastic lesions related to the time intervals of the examination is shown in Figure 4. The preneoplastic lesions (LCD and BLCN) start to appear in TT mice 100 days after DENA inoculation and reach a peak at 300 days. The neoplastic lesions (HA and HC) arise in TT mice after 200 days from treatment with DENA and reach a peak at 400 days, following the peak of the preneoplastic lesions.

Vascular Lesions of the Liver

Dilatations of liver sinusoids and central veins, with the characteristics of vascular ectasis, were observed only in the first experiment, with no significant difference between TT and CC mice. This condition may be related to hemodynamic modifications as a consequence of liver cell necrosis induced by DENA. Two and four emangiomas were observed in TT and CC livers, respectively. They consisted of irregularly branching vessels, spaces, and lacunae lined by flat endothelial cells with fibrous septa, sometimes containing compressed and atrophic liver cells. Endothelial cells showed normal nuclei and no mitoses. Thrombosis and scarring were common.

Figure 2. Liver cell proliferative lesions. **A** and **B:** LCD. Lobular architecture is retained with the portal tract and central vein normally located. Dysplastic hepatocytes show nuclear pleomorphism and are often binucleated. H&E; original magnifications, ×63 (**A**), ×400 (**B**). **C** and **D:** BLCN. Foci of dysplastic hepatocytes with basophilic cytoplasm surround frequently the central vein; no sharp outline separates the abnormal foci from adjacent normal hepatocytes. H&E; original magnifications, ×25 (**C**), ×160 (**D**). **E** and **F:** HA. The adenoma compresses surrounding normal liver cells; plates of neoplastic hepatocytes form trabeculae separated by sinusoid-like vessels. Nuclear atypia and mitoses are evident. H&E; original magnifications, ×160 (**E**), ×400 (**F**). **G:** HA. Electron micrograph illustrating the fine structure of adenoma cells. S, sinusoidal surface; **arrowhead**, bile canaliculus. The Disse space is reduced and adenoma cells lack microvilli. Bile canaliculus is irregularly dilated with few and thick microvilli. Original magnification, ×3000.

Table 1. Frequency of TT and CC Affected Animals According to the Different Treatments with DENA

DENA treatment	Animals with lesions	Total lesions observed	Animals without lesions
TT mice, 1st experiment	64/64 (100%) M:31-F:33	162	0
TT mice, 2nd experiment	25/25 (100%) M:11-F:14	57	0
CC mice, 1st experiment	45/150 (30%) M:22-F:23	124	105
CC mice, 2nd experiment	13/50 (26%) M:9-F:4	34	37

TT, tat-transgenic mice; CC, control BDF mice; M, male; F, female.

Extra-Hepatic Lesions

Alterations outside the liver had a low frequency both in TT (36.1%) and in CC (26.7%) animals. Proliferative and neoplastic lesions of the lung are likely caused by the carcinogenic action of DENA and no significant differences were observed between TT and CC mice. Lymphomas were observed only in TT mice and may be directly related to the transgenic status, because TT mice spontaneously develop such tumors.[15,16]

Lung Lesions

Lung lesions were of two types with a low frequency in both experiments: 1) small nodular hyperplastic proliferations (10.1% in TT and 6.0% in CC mice) with a solid or papillary growth pattern and with ill defined outlines from the adjacent lung tissue; 2) adenocarcinomas (4.5% in TT and 1.6% in CC mice) of variable size with irregular and infiltrating margins. The first lesions were made up by trabeculae and cords containing epithelial cells larger than normal pneumocytes and epithelial bronchiolar cells, showing central round nucleus and small nucleoli, irregularly distributed. No mitoses were observed. The nodular tumors showed nests and cords of more atypical epithelial cells extending into the parenchyma with an altered nuclear/cytoplasmic ratio, vesicolous nuclei, and evident macronucleoli. Mitoses were frequent. The lung tissue adjacent to the proliferative lesions showed capillary congestion and numerous macrophages in the alveolar lumens. Bronchial tubes showed foci of epithelial hyperplasia with increase of eosinophilic bronchial cells.

Lymphomas, Adenocarcinomas, and Leiomyosarcomas

Lymphomas were 4.6% in DENA-treated TT mice and consisted of large blastic cells mixed to more mature and differentiated cells such as lymphocytes and plasma cells and other intermediate lymphoid cells. By histochemical analysis, large blastic cells expressed CD19, CD20, CD21, and CD45R (4KB5) B cell markers. These characteristics indicate that these tumors are B cell lymphomas which were observed to develop spontaneously at the frequency of 7% in TT mice.[15,16] No lymphomas were detected in DENA-treated CC mice. Adenocarcinomas and leiomyosarcomas of the skin were found at the same frequency in DENA-treated TT mice as reported previously in TT mice.[15,16] The same incidence of lymphomas, adenocarcinomas, and leiomyosarcomas in DENA-treated TT mice as in TT mice suggests that these tumors are not related to the carcinogenic activity of DENA.

Non-Neoplastic Lesions

The non-neoplastic lesions were skin ulcers; amyloid depositions in the liver, kidneys, and spleen; and chronic pyelonephritis with hydronephrosis, often associated with amyloid as reported previously.[15,16] Skin lesions were very similar to those found in TT mice.[15,16]

Amyloidosis

Systemic amyloidosis represented the most frequent non-neoplastic and nonspecific alteration observed in TT as well as in CC animals. It was always associated with chronic inflammation of the skin, kidneys, and liver or of the pelvic organs in females. Amyloid substance depositions were commonly found in the liver, kidneys, and spleen, less frequently in the small intestine wall and in lymph nodes.

Table 2. Incidence of Hepatic Lesions in TT and CC Mice

Hepatic lesions	TT mice		CC mice		*P* value
	Animals with lesions	Percentage	Animals with lesions	Percentage	
First experiment					
LCD	19/64	29.7	19/150	12.7	3.3×10^{-3}
BLCN	37/64	57.9	35/150	23.3	1.5×10^{-6}
HA	26/64	40.6	15/150	10.0	6.6×10^{-7}
HC	32/64	50.0	19/150	12.7	1.7×10^{-8}
Second experiment					
LCD	14/25	56.0	6/50	12.0	9.7×10^{-5}
BLCN	9/25	36.0	11/50	22.0	1.5×10^{-1}
HA	8/25	32.0	4/50	8.0	1.1×10^{-2}
HC	8/25	32.0	2/50	4.0	1.7×10^{-3}

TT, tat-transgenic mice; CC, control BDF mice; LCD, liver cell dysplasia; BLCN, basophilic liver cell nodules; HA, hepatocellular adenomas; HC, hepatocellular carcinomas. *P* value was obtained by Fisher's exact test.

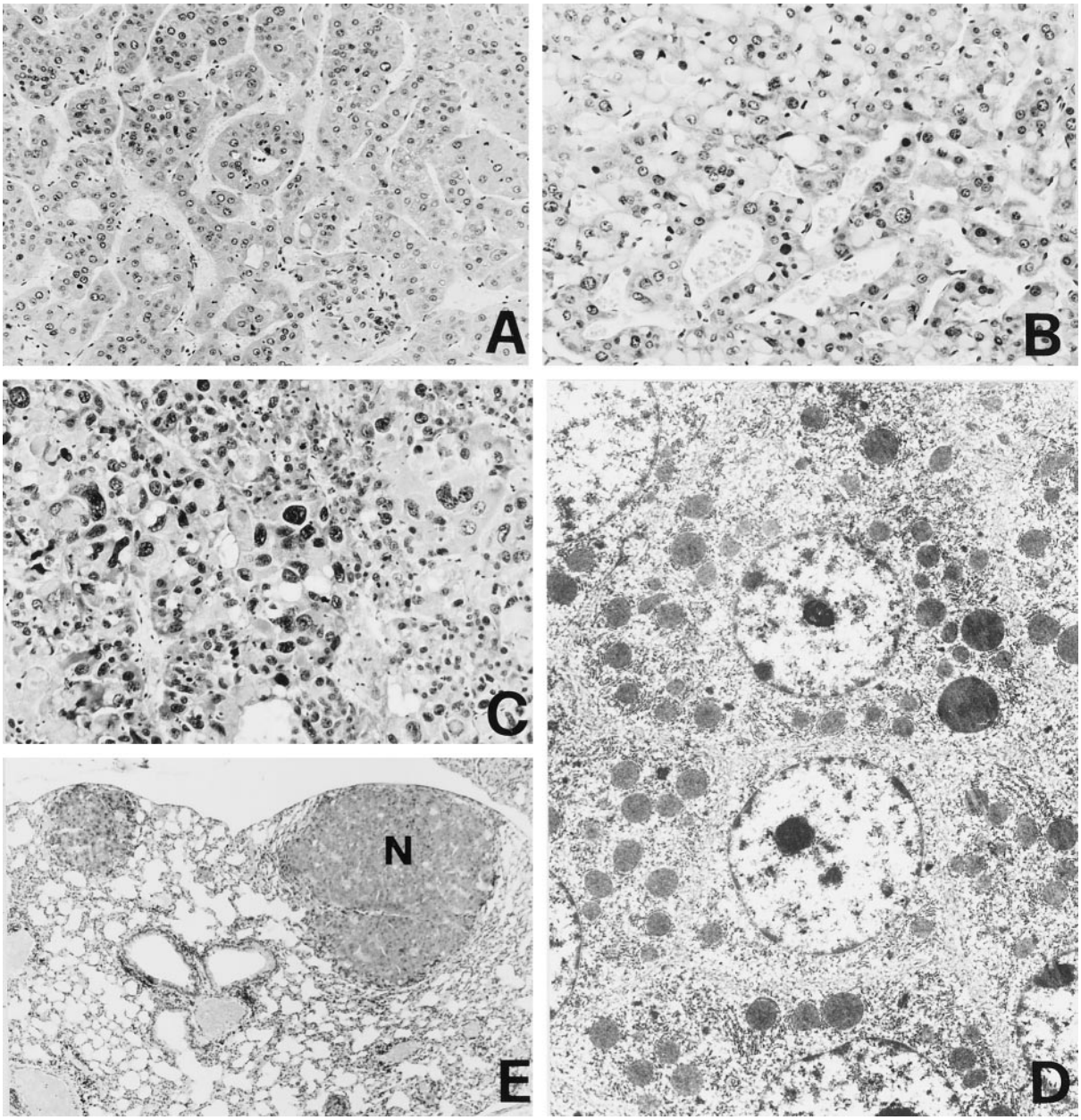

Figure 3. HC. **A:** Trabecular pattern with cords of neoplastic cells showing acinar or pseudoglandular structures. **B:** Neoplastic hepatocytes contain hyaline inclusions in the cytoplasm. **C:** Solid poorly differentiated carcinoma with great variability of nuclei showing giant polynucleated cells and necrosis. **D:** Electron micrograph showing the fine structure of a differentiated hepatocarcinoma: neoplastic cells are not polarized; no bile canaliculus is evident. **E:** Nodular metastases (N) of HC in lung tissue. H&E; original magnifications: ×160 (**A**), ×250 (**B**), ×400 (**C**), ×25 (**E**), and ×2500 (**D**).

Chronic Inflammatory Lesions

Hydronephrosis was constantly associated with chronic pyelonephritis and interstitial fibrosis of the kidneys; the grade of parenchymal atrophy was variable but sometimes severe.

Discussion

TT mice, where the HIV-1 *tat* gene is expressed in all tissues and organs, develop a number of neoplastic phenotypes.[15,16] These tumors and preneoplastic lesions appear both in transgenic and control animals, but with significantly greater frequency, more severity, and earlier in life in the transgenic group,[15,16] suggesting that *tat* expression is supporting and activating a natural predisposition of these animals to develop such lesions. TT mice show proliferative liver lesions at high frequency.[14–16,26] In BKV/TT mice, the incidence of HC is low, but most animals show a diffuse LCD.[15,16] We therefore chose to treat BKV/TT mice with DENA, a hepatotropic carcinogen, to assess whether Tat-induced LCD predisposes these animals to liver carcinogenesis. The results showed that both DENA-induced preneoplastic lesions (LCD and BLCN) and liver tumors (HA and HC) were significantly more frequent in TT than in CC animals. Moreover, during

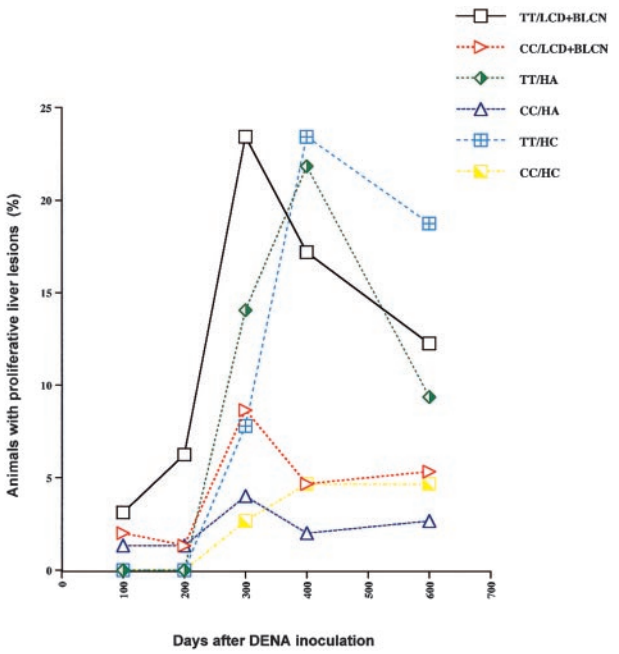

Figure 4. Incidence of proliferative liver lesions in mice treated with two DENA inoculations, related to the time of examination.

the course of the experiments, the development of LCD and BLCN in TT mice preceded the peak of HA and HC, suggesting that in TT mice Tat expression in the liver favors progression of the preneoplastic to the neoplastic phenotype, thus leading to a greater frequency of malignant tumors. The *tat* transgene was detected and expressed in preneoplastic and neoplastic tissues, supporting a pathogenetic role for Tat in the development of such lesions.

DENA is a potent initiator carcinogen which induces hepatic necrosis early after administration. The ensuing regenerative process, involving proliferation of hepatocytes, is accompanied by chromosome alterations and mutations, leading to the appearance of preneoplastic cells that gradually evolve toward a malignant phenotype. The constitutive expression of Tat in liver of TT mice may therefore support the carcinogenic effect of DENA in two ways: 1) the presence of Tat-induced LCD enhances the genetic alterations accompanying liver regeneration after the necrotic activity of DENA, contributing to the initiation of the neoplastic phenotype; and 2) the effect of Tat-promoting cell proliferation stimulates the expansion of neoplastic clones, accompanied by acquisition of additional genetic alterations, thus favoring progression to malignancy of the early neoplastic lesions. This effect of Tat on hepatocyte proliferation and malignant progression is most likely because of its anti-apoptotic activity,[11,12] angiogenic functions,[9,10] and ability to induce expression of growth factors,[8,12] cytokines,[27,28] and transcription factors.[29] In addition, LCD in *TT* mice is associated to aneuploidia which is a manifestation of genetic instability,[30] one of the main factors of progression to malignancy in human tumors.[31] Our results are in agreement with predisposition to chemical carcinogenesis in other models of genetically modified mice. In fact, Li et al[18] demonstrated an enhanced carcinogenic effect of DMBA in mice transgenic for a mutant p53 gene and predisposition to urethan-induced carcinogenesis was shown in mice bearing a transgenic hepatitis B virus genome.[17] In addition, Kemp et al[19] reported that knock-out mice heterozygous or nullizygous for p53 show an accelerated progression of epidermal hyperplasia, induced by 9,10-dimethyl-1,2-benzanthracene and 12-O-tetradexanoyl phorbol-13-acetate, to adenoma and squamous cell carcinoma.

This study indicates that preneoplastic conditions established by Tat may contribute to initiation and progression of the tumorigenic process. These results may have an important implication for the neoplastic pathology observed in the course of AIDS. Indeed, extracellular Tat, taken up by normal cells of HIV-1-infected patients,[4–7] may predispose these cells to the oncogenic effect of exogenous and endogenous carcinogens. These results also suggest that reasonable efforts should be developed to inhibit Tat oncogenic activity in HIV-1-infected patients with immunoprophylactic,[32] immunotherapeutic, and gene therapy approaches.[13]

Acknowledgments

We thank A. Bevilacqua, I. Pivanti, A. L. Peverati, P. Zucchini, C. Lanza, and V. Lazzarin for excellent technical assistance; L. Rinaldi and A. Leorin for photographs; and Dr. C. Conighi for statistical analysis.

References

1. Beral V, Jaffe H, Weiss R: Cancer, HIV and AIDS. Cancer Surv 1991, 10:1–3
2. Biggar RJ: Cancer in the acquired immunodeficiency syndrome: an epidemiological assessment. Semin Oncol 1990, 17:251–260
3. Cremer KJ, Spring SB, Gruber J: Role of human immunodeficiency virus type 1 and other viruses in malignancies associated with acquired immunodeficiency syndrome. J Natl Cancer Inst 1990, 82: 1016–1025
4. Ensoli B, Buonaguro L, Barillari G, Fiorelli V, Gendelman R, Morgan RA, Wingfield P, Gallo RC: Release, uptake, and effects of extracellular human immunodeficiency virus type 1 Tat protein on cell growth and viral transactivation. J Virol 1993, 67:277–287
5. Chang HC, Samaniego F, Nair BC, Buonaguro L, Ensoli B: HIV-1 tat protein exits from cells via a leaderless secretory pathway and binds to extracellular matrix-associated heparan sulfate proteoglycans through its basic region. AIDS 1997, 11:1421–1431
6. Frankel AD, Pabo CO: Cellular uptake of the Tat protein from human immunodeficiency virus. Cell 1988, 55:1189–1193
7. Helland DE, Welles JL, Caputo A, Haseltine WA: Transcellular transactivation by the human immunodeficiency virus type 1 Tat protein. J Virol 1991, 65:4547–4549
8. Ensoli B, Barillari G, Salahaudin ZS, Gallo RC, Wong-Staal F: Tat protein of HIV-1 stimulates growth of cells derived from Kaposi's sarcoma lesions of AIDS patients. Nature 1990, 345:84–86
9. Ensoli B, Gendelman R, Markham P, Fiorelli V, Colombini S, Raffeld M, Cafaro A, Chang HK, Brady J, Gallo RC: Synergy between basic fibroblast growth factor and HIV-1 Tat protein in induction of Kaposi's sarcoma. Nature 1994, 371:674–680
10. Albini A, Barillari G, Benelli R, Gallo RC, Ensoli B: Tat, the human immunodeficiency virus type regulatory protein, has angiogenic properties. Proc Natl Acad Sci USA 1995, 92:4838–4842
11. Zauli G, Gibellini D, Milani D, Mazzoni M, Borgatti P, La Placa M, Capitani S: Human immunodeficiency virus type 1 Tat protein protects lymphoid, epithelial, and neuronal cell lines from death by apoptosis. Cancer Res 1993, 53:4481–4485

12. Campioni D, Corallini A, Zauli G, Possati L, Altavilla G, Barbanti-Brodano G: HIV type 1 extracellular Tat protein stimulates growth and protects cells of BK virus/*tat* transgenic mice from apoptosis. AIDS Res Hum Retroviruses 1995, 11:1039–1048
13. Caputo A, Betti M, Boarini C, Mantovani I, Corallini A, Barbanti-Brodano G: Multiple functions of human immunodeficiency virus type 1 Tat protein in the pathogenesis of AIDS. Recent Research Developments in Virology. Edited by SG Pandalai. Trivandrum, Transworld Research Network, 1999, pp 753–771
14. Vogel J, Hinrichs SH, Reynolds RK, Luciw PA, Jay G: The HIV *tat* gene induces dermal lesions resembling Kaposis's sarcoma in transgenic mice. Nature 1988, 355:606–611
15. Corallini A, Altavilla G, Pozzi L, Bignozzi F, Negrini M, Rimessi P, Gualandi F, Barbanti-Brodano G: Systemic expression of HIV-1 *tat* gene in transgenic mice induces endothelial proliferation and tumors of different histotypes. Cancer Res 1993, 53:5569–5575
16. Altavilla G, Trabanelli C, Merlin M, Caputo A, Lanfredi M, Barbanti-Brodano G, Corallini A: Morphological, histological, immunohistological, and ultrastructural characterization of tumors and dysplastic and non-neoplastic lesions arising in BK virus/*tat* transgenic mice. Am J Pathol 1999, 154:1231–1244
17. Dragani TA, Manenti G, Farza H, Della Porta G, Tiollais P, Pourcel C: Transgenic mice containing hepatitis B virus sequences are more susceptible to carcinogen-induced hepatocarcinogenesis. Carcinogenesis 1990, 11:953–956
18. Li B, Murphy KL, Laucirica R, Kittrell F, Medina D, Rosen JM: A transgenic mouse model for mammary carcinogenesis. Oncogene 1998, 16:997–1007
19. Kemp CJ, Donehower LA, Bradley A, Balmain A: Reduction of p53 gene dosage does not increase initiation or promotion but enhances malignant progression of chemically induced skin tumors. Cell 1993, 74:813–822
20. Craddock VM: Effect of a single treatment with the alkylating carcinogens dimethylnitrosamine, diethylnitrosamine and methylmethanesulphonate on liver regenerating after partial hepatectomy. Test for induction of liver carcinomas. Chem Dial Interact 1975, 10:313–321
21. Solt DB, Medline A, Farber E: Rapid emergence of carcinogen-induced hyperplastic lesions in a new model for the sequential analysis of liver carcinogenesis. Am J Pathol 1977, 88:595–618
22. Vesselinovitch SD, Mihailovich N: Kinetics of diethylnitrosamine hepatocarcinogenesis in the infant mouse. Cancer Res 1983, 43:4253–4259
23. Koen H, Pugh T, Goldfarb S: Hepatocarcinogenesis in the mouse. Combined morphologic-stereologic studies. Am J Pathol 1983, 112: 89–100
24. Becker FF: Morphological classification of mouse liver tumors based on biological characteristics. Cancer Res 1982, 42:3918–3923
25. Sambrook J, Fritsch EF, Maniatis T: Molecular Cloning: A Laboratory Manual, ed 2. Cold Spring Harbor, Cold Spring Harbor Laboratory Press, 1989
26. Vogel J, Hinrichs SH, Napolitano LA, Ngo L, Jay G: Liver cancer in transgenic mice carrying the human immunodeficiency virus *tat* gene. Cancer Res 1991, 51:6686–6690
27. Scala G, Ruocco MR, Ambrosino C, Mallardo M, Giordano V, Baldassare F, Dragonetti E, Quinto I, Venuta S: The expression of the interleukin 6 gene induced by the human immunodeficiency virus type 1 Tat protein. J Exp Med 1994, 179:961–971
28. Westendorp MO, Li-Weber M, Frank RW, Krammer PH: Human immunodeficiency virus type 1 upregulates interleukin secretion in activated T cells. J Virol 1994, 68:4177–4185
29. De Marchi F, d'Adda di Fagagna F, Falaschi A, Giacca M: Activation of transcription factor NF-κB by the Tat protein of human immunodeficiency virus type-1. J Virol 1996, 70:4427–4437
30. Li R, Yerganian G, Duesberg P, Kraemer A, Willer A, Rausch C, Hehlmann R: Aneuploidy correlated 100% with chemical transformation of Chinese hamster cells. Proc Natl Acad Sci USA 1997, 94: 14506–14511
31. Lengauer C, Kinzier KW, Vogelstein B: Genetic instabilities in human cancers. Nature 1998, 396:643–649
32. Cafaro A, Caputo A, Fracasso C, Maggiorella MT, Goletti D, Baroncelli S, Pace M, Sernicola L, Koanga-Mogtomo ML, Betti M, Borsetti A, Belli R, Akerblom L, Corrias F, Buttò S, Heeney J, Verani P, Titti F, Ensoli B: Control of SHIV-89.6P-infection of cynomolgus monkeys by HIV-1 Tat protein vaccine. Nature Med 1999, 5:643–650